Knockdown analysis of the performance of solar photovoltaic plants

Siddhartha Bhatt M*

This paper presents an efficiency map of a solar photovoltaic (SPV) plant through knock down analysis for the three major cell types monocrystalline silicon (C-Si), multicrystalline (M-Si) and amorphous silicon (A-Si). The highest efficiency achievable by a SPV cell is the Shockley-Queisser (SQ) limit which is the ultimate efficiency. When it comes to computing the working cell efficiency which can be treated as the SQ nominal conditions (after considering the cell losses) there is a drop. Moving up the organizational level, while at the module level, there is a further drop in the overall efficiency by 2-3 % points between the cell and the module. Further drop is seen when computing under Standard test conditions (STC) conditions and (PTC conditions PV-USA industrial test conditions). The STC module efficiency is taken as the reference or base condition for the SPV plant design. From the module to the array there is yet a drop of 3-4 % points. The performance drop of the plant from the STC conditions to the actually achieved conditions can be represented by the performance ratio (PR) which considers the stochastic efficiency of the plant site. The PR excludes excludes auxiliary power (2-4 % of the generated power), losses in battery (~20 %) due to storage component (if storage is present) and loss of energy generated due to non-availability of the grid (for grid tied systems). The stochastic incident radiation loss (~16-37 %) is already accounted in the PR. Automation helps to a large extent in tracking the component efficiencies and correcting the losses.

The paper also covers the sensitivity of SPV efficiency to positive factors such as incident angle variation, module tracking, Maximum Power Point Tracking (MPPT), concentration, etc., and negative factors such as environmental conditions (temperature, turbidity, water vapor), cell shunt resistance, initial and long term degradation, etc..

Keywords *: Solar photovoltaic, system efficiency, SQ efficiency, performance ratio, cell efficiency, module efficiency, array efficiency, plant efficiency.*

1.0 INTRODUCTION

An SPV with both crystalline silicon (mono- and poly-cells) (C-Si, M-Si) and amorphous (thin film) (A-Si) converters are emerging as the largest capacity addition source [30-32 GWp (GWp indicates the maximum power rating at 1200 hours) in 2012] in a given year in the human history. The world capacity of SPV is over 150 GW and the annual production capacity is 30-40 GWp/year. Many new countries are going in for SPV adoption at a compound annual growth rate (CAGR) of 20-50 %. In India the capacity is around 3 GWp and likely to increase to around 20 GWp in 2020 with a present manufacturing capacity of 1 GWp/year which is on the upsurge to 3 GWp/year. The cost of SPV has dropped to Rs. 45/Wp. At this juncture, the concern in SPV is to improve the overall efficiency and capacity utilization of the plant; and reducing the size of the unit (capital cost).

Since solar radiation varies over the day (0600 to 1800 hours) from 0 to 1,000 W/m2, the average load factor of solar plants over a day (24 hours) is normally within 25 % of the peak power unlike conventional generation which can achieve load factors of 100 % over a given time period. The conversion efficiencies of single junction SPV cells are limited by the Shockley-Queisser (SQ) limit of 31 % without concentration and 41 % under concentration [1]. The overall efficiency of SPV cells and modular architecture constructed out of them, viz., modules, panels, arrays and plants can be increased by improvement in the cell and associated system efficiency as follows:

- Improvement in cell photovoltaic efficiency

  ✓ Multi-junction cells.

  ✓ III-IV multispectral cells.

  ✓ Light trapping structures with transparent top conductor and bottom electrode.

  ✓ Intermediate band solar cells with high radiative energy.

  ✓ Quantum dot SPV.

  ✓ Thermo photovoltaics (TPV) to overcome SQ barrier.

  ✓ Concentrated radiation SPV.

- Improvement in cell thermodynamic efficiency

  ✓ Trigeneration- SPV for power generation, thermal energy for heating and cooling.

  Improvement in system efficiency

  ✓ Photopic efficiency.

  ✓ Electrical efficiency.

Presently, SPV systems are used in three configurations:

- Off grid power generation systems with battery energy storage for autonomy.

- Grid connected systems without battery energy storage operating in the anti islanding mode.

Grid connected systems with battery energy storage for islanded operation during grid failure periods

2.0 REVIEW OF IMPROVEMENT IN SPV SYSTEM EFFICIENCY

Green *et al.* [2] have cone out with a comprehensive listing of confirmed efficiencies of C-Si, M-Si and A-Si cells and modules under standard conditions. Aste *et al.* (2014) [3] have evaluated the outdoor performance of C-Si, M-Si and A-Si modules in temperature zones. They have used the Performance Ratio (PR) factor for correlating the reference standard performance and the annual field performance.

Molecular SPV cells are presently showing modest efficiencies of 3 % but hold promise as a future alternative because of superiority in interfacial recombination and mobility losses [4]. Quantum dot SPV through specially tuned solution processes using plasmonic nanoparticles show 35 % increase in SPV efficiency in the near IR region and 11 % increase in the overall solar spectrum [5].

Concentrated triple junction SPV cells need to be optimized with respect to grid pitch (pitch of the grid electrodes) [6]. Maximum efficiency of 39.5 % was observed for systems with CRs of 250-1000 for grid pitch of 100-150 μm [6].

A SPV unit with five single junction photocells with four optical filters which divide the spectrum into five regions with a CR of 2.8 and 3.8 recorded efficiencies of 35.6 % and 42.7 % respectively [7]. This is nearly 81 % of the theoretical limit of individual segment efficiencies.

Solar thermal photovoltaic (TPV) attempts to overcome the SQ barrier using low band gap materials. The SPV efficiency can be decoupled into intermediate efficiency which is the total power radiated by the emitter to the total incident radiation; and cell efficiency is the electrical power extracted by the cell to the total power radiated by the emitter [8]. Intermediate efficiency is

improved through solar TPV systems. According to [9], 30 % improvement is possible through solar TPV.

Considering the sun as a heat source at Ts= 5778 K and the heat sink at T_0=300 K, the maximum convertible fraction of energy (Carnot efficiency) is,

$$\eta = \left[1 - \left(\frac{T_0}{T_s}\right)\right] x100 = 94.80\ \% \qquad ....(1)$$

This level of efficiency (94.8 %) is limited by the SQ limits. Trigeneration aims at converting part of the thermal energy into cooling effect and part of the thermal energy as useful heat. Trigeneration technologies are significant to SPV plants installed in residential or commercial buildings with cooling loads and heating loads. Instead of using the electrical power from SPV for servicing heating and cooling loads, these can directly be met from the waste thermal energy generated in SPV plants.   The extraction of thermal energy from SPV plants has a positive effect on the power generation potential as loss of power due to temperature effect is decreased. Thermal energy is extracted for cooling through thermoelectric coolers and for heating through heat pipes or directly through fluid flow in coils below the SPV panels. Tri-generation using SPV roof top has been applied to individual cottage type buildings resulting in reduction in electrical energy for cooling and heating requirement [10].

High energy efficiency concentrated triple junction SPV with disk type concentrators to operate two effect absorption chillers, thermal energy from the concentrator and electrical power has been established [11]. Tri-generation based on coupling SPV with vapor compression heat pumps for heating and cooling have been proved [12]. Electrical powered heating and cooling loads is replaced by direct coupled heating and cooling while electrical output of SPV is used only for lighting, communication and motor loads.

3.   COMPARATIVE PERFORMANCE PARAMETERS

3.1   Cell theoretical efficiency (Shockley Queisser limit)

$$\eta_{SQ,n} = \eta_{SQ,u}\eta_{QInt}\eta_{QC}\frac{E_G\int_0^{\lambda_G}\Phi^0(\lambda)d\lambda}{\int_0^{\lambda_G}\Phi^0(\lambda)\frac{hc}{\lambda}d\lambda}\frac{\int_0^{\lambda_G}\Phi^0(\lambda)\frac{hc}{\lambda}d\lambda}{\int_0^{\infty}\Phi^0(\lambda)\frac{hc}{\lambda}d\lambda}\eta_{Qe}\eta_\rho(1-\rho)\frac{A_f}{A_{tot}}\frac{qV_{oc}}{E_G}\eta_J\eta_R FF...(2)$$

$\eta_{SQ,n} =$

$\eta_1\eta_2\,\eta_3\,\eta_4\,\eta_5\,\eta_6\,\eta_7\,\eta_8\eta_9\,\eta_{10}\,\eta_{11}\,\eta_{12}...(3)$

$$\eta_{SQ,n} = \frac{V_{oc}I_{sc}}{P_I}$$

$\eta_{SQ,n}$ = Shockley Queisser nominal efficiency

V_{oc}= open circuit voltage of cell ,V

I_{sc}= short circuit current of cell ,A

$\eta_1 = \eta_{SQ,u}$ = Efficiency due to band gap loss

$$\eta_{SQ,u} = \frac{h\nu_g(\phi_{incident} - \phi_{radiative})}{P_I}$$

The theoretical limit for solar cells (single pn junction) is given by the celebrated Shockley -Queisser (SQ) ultimate efficiency.   The SQ upper limit which is described as ultimate efficiency is multiplied by the detailed balance efficiency which takes into account the emission and absorption and emission of photons in the cell [13]. Liao and Hsu [14] have investigated the SQ efficiency for single pn junctions and have developed a transcendental equation which can be solved for various energy band gaps and temperatures assuming impedance matching factors.

The limiting efficiency drops in the conversion efficiency using the SQ limit as the starting point have been given in detail [15]. The break up of nominal efficiency into ultimate efficiency and detailed balance efficiency   has been used for computing the efficiency limits of solar cells

over the band gap [16]. Jha [17] has described several loss evaluation schemes for computing the energy efficiency of solar cells taking into consideration the unmatched spectral response, band gap losses, fill factor, reflection, etc.

The nominal SQ efficiency   is calculated as, $\eta_{SQ,n}$ = efficiency due to band gap loss

$$\frac{qV_g(\emptyset_{incident} - \emptyset_{radiati}}{\sigma \epsilon (T_s^4 - T_o^4)} \qquad \text{....(4a)}$$

$\eta_{SQ,u}$ = Shockley Queisser nominal efficiency

P_I = Incident solar radiation, W/m²

$h\nu_g$ = band gap energy, eV

$\lambda_g = 1/\nu_g$ = wavelength of photons that corresponds to the band gap energy of the absorber of the solar cell

h = Planck's constant, m² kg/s

q = unit electric charge= 1.602 x 10⁻¹⁹ C

V_g = band gap voltage

$\emptyset_{incident}$ = incident photon flux, photons.m⁻²s-1

$\emptyset_{radiative}$ = radiative photon flux, photons.m⁻²s⁻¹

σ = Stefan Boltzmann constant (5.67 × 10⁻⁸ W/m² k⁴)

$\in$ = emissivity of the incident surface (-)

T_s = temperature of the source (sun) (K)

T_o = sink temperature (K)

$\eta_2 = \eta_{QInt}QC$ = Loss by incomplete absorption due to the finite thickness

η_{QInt} = Internal quantum efficiency = Probability that a photon is absorbed in a material

η_{Qc} = Quantum efficiency for carrier station = No. of electron hole pairs generated by the absorbed photon

$$\eta_{QInt} = \frac{\eta_{Qext}}{(1 - \gamma - \tau)} \qquad \text{....(4b)}$$

$1 = \rho + \tau + \gamma$

γ = Reflectance

τ = Transmittance

$\eta_{QInt} = \dfrac{\textit{No. of electrons generated by the device}}{\textit{No. of photons}}$

$$\eta_3 = \frac{E_G \int_0^{\lambda G} \Phi^0(\lambda)d\lambda}{\int_0^{\lambda G} \Phi^0(\lambda)\frac{hc}{\lambda}d\lambda}$$ = Efficiency to account for loss due to thermalization of the excess energy of photons

λ = Wavelength of incident solar radiation, nm

c = Velocity of light, 3 × 10⁸ m/s

$$\eta_4 = \frac{\int_0^{\lambda G} \Phi^0(\lambda)\frac{hc}{\lambda}d\lambda}{\int_0^{\infty} \Phi^0(\lambda)\frac{hc}{\lambda}d\lambda} =$$ Efficiency to account for loss due to non-absorption of long wavelengths = Spectral mismatch factor in simulator as compared to reference or normal radiation.

The spectral mismatch is around 3 % [19] and can go up to 7 %.

$\eta_5 = \eta_{Qe}$ = Electrical quantum efficiency =Probability that a photon generated carrier is collected

$\eta_6 = (\rho)$ = Efficiency due to absorptivity on cell surface

$\eta_7 = (1-\rho)$ = Loss due to total reflection of light

ρ = Absorptance

$\eta_8 = \frac{A_f}{A_{tot}}$ = Area ratio= Loss due to shading and coverage by metal electrodes

$\eta_9 = \frac{qV_{oc}}{E_G}$ = Efficiency to indicate for loss due to voltage factor

$\eta_{10} = J$ = Junction efficiency due to geometric parameter and dimension

$\eta_{11} = R$ = Efficiency due to contact resistance

$\eta_{12} = FF$ = Fill Factor

Figures 1 and 2 and give the standard solar spectral direct and diffuse irradiance as per ASTM [18]. In the presence of all components, the spectral curve follows the black body characteristic. Figure 3 gives the range of variation of the conversion efficiency of SPV cells for respective band gaps. Table 1 gives the break down of the efficiencies due to various losses.
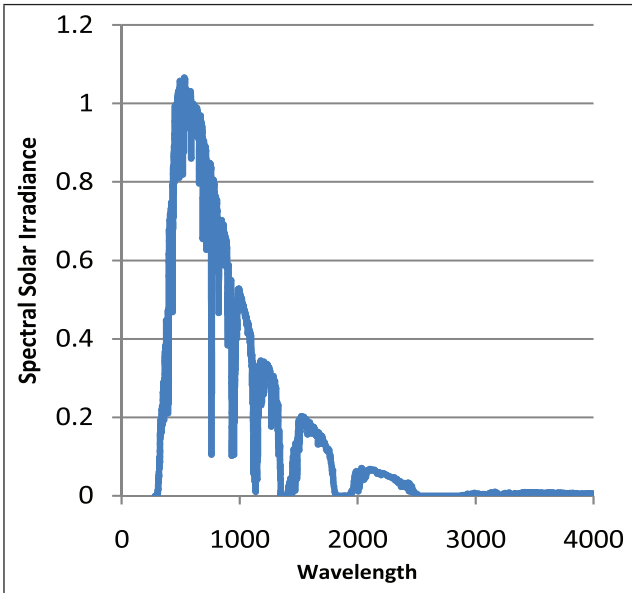

FIG. 1   STANDARD SOLAR SPECTRAL DIRECT IRRADIANCE AS PER ASTM
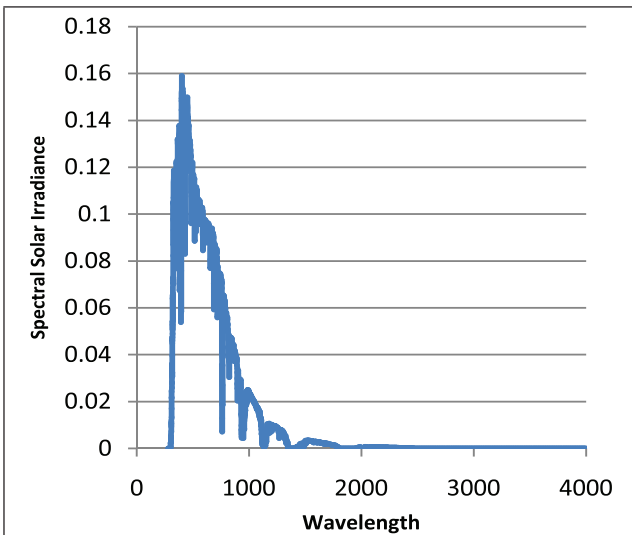

FIG. 2   STANDARD SOLAR SPECTRAL DIRECT IRRADIANCE AS PER ASTM

Spectral mismatch on a clear day without appearance of cloud cover is quite low (below 2 %) but can increase to 7 % when there are environmental fluctuations of irradiance.
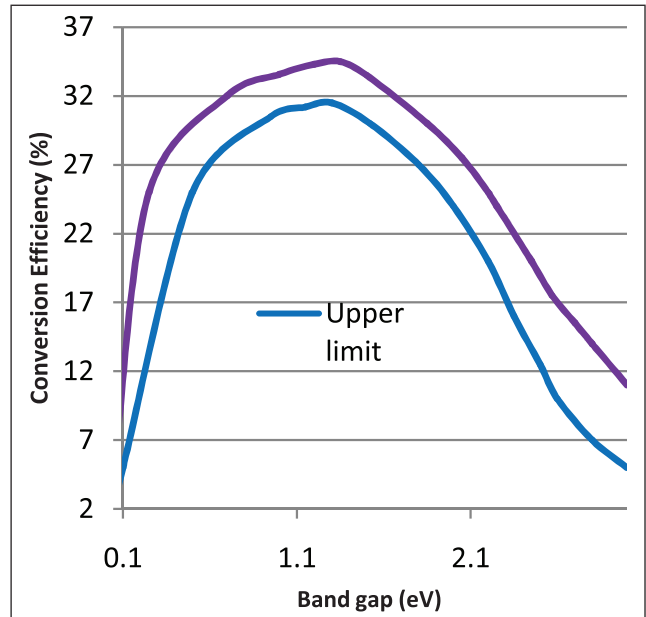

FIG. 3   RANGE OF VARIATION OF THE CONVERSION EFFICIENCY OF SPV CELLS

TABLE 1			
BREAK DOWN OF THE EFFICIENCIES DUE TO VARIOUS LOSSES			
Sl. No.	Particulars	Symbol	Value
1	Shockley Queisser ultimate efficiency	$\eta_{SQ,u}$	47
2	Efficiency due to band gap loss	η_1	0.93
3	Loss by incomplete absorption due to the finite thickness	η_2	0.98
4	Efficiency to account for loss due to thermalization of the excess energy of photons	η_3	0.94
5	Efficiency to account for loss due to non-absorption of long wavelengths and unmatched spectral response	η_4	0.93
6	Electrical quantum efficiency	η_5	0.96
7	Efficiency due to absorptivity on cell surface	η_6	0.98

8	Loss due to total reflection, deflection and shadows	η_7	0.91
9	Area ratio	η_8	0.90
10	Efficiency to indicate for loss due to voltage factor	η_9	0.95
11	Junction efficiency due to geometric parameter and dimension	η_{10}	0.86
12	Efficiency due to contact resistance	η_{11}	0.98
13	Fill Factor	η_{12}	0.85
14	Shockley Queisser nominal efficiency	$\eta_{SQ,n}$	18.17

3.2 Performance measuring conditions - stc and ptc conditions

STC (Standard test conditions) refer to an irradiance of 1 sun (1,000 W/m²), a cell temperature of 25°C, an air mass of 1.5, and standard spectrum as per ASTM G173-03 [18]. PTC (PV-USA test conditions) (industrial) refer to an irradiance of 1 sun (1,000 W/m²),   a cell temperature of 20°C, a wind speed of 1 m/s above ground level and standard spectrum as per ASTM G173-03 [18].   STC and PTC tests on modules are done with a xenon flash tube.

Agroui *et al.* [19] have given the conversion formulae for   conversion of measurement data from environmental operating conditions (EOC) to STC conditions   for I_{SC}, V_{OC}, I-V curve and P_{max} using three different methods, viz., IEC 60981 (valid over irradiance of 700 W/m² and module temperature of 35-50 °C), Anderson's method (irradiance of 100-1,000 W/m² and module temperature of 25-75 °C), and Blaesser's method (for C-Si for irradiance of > 700 W/m²). These formulae are valid over the whole range of solar irradiance.

Figure 4 shows the drop from STC to PTC for over 16,000 data points. The R^2 shows a low value indicating that   the average drop from 1.0 to 0.885 is independent of the module output power.

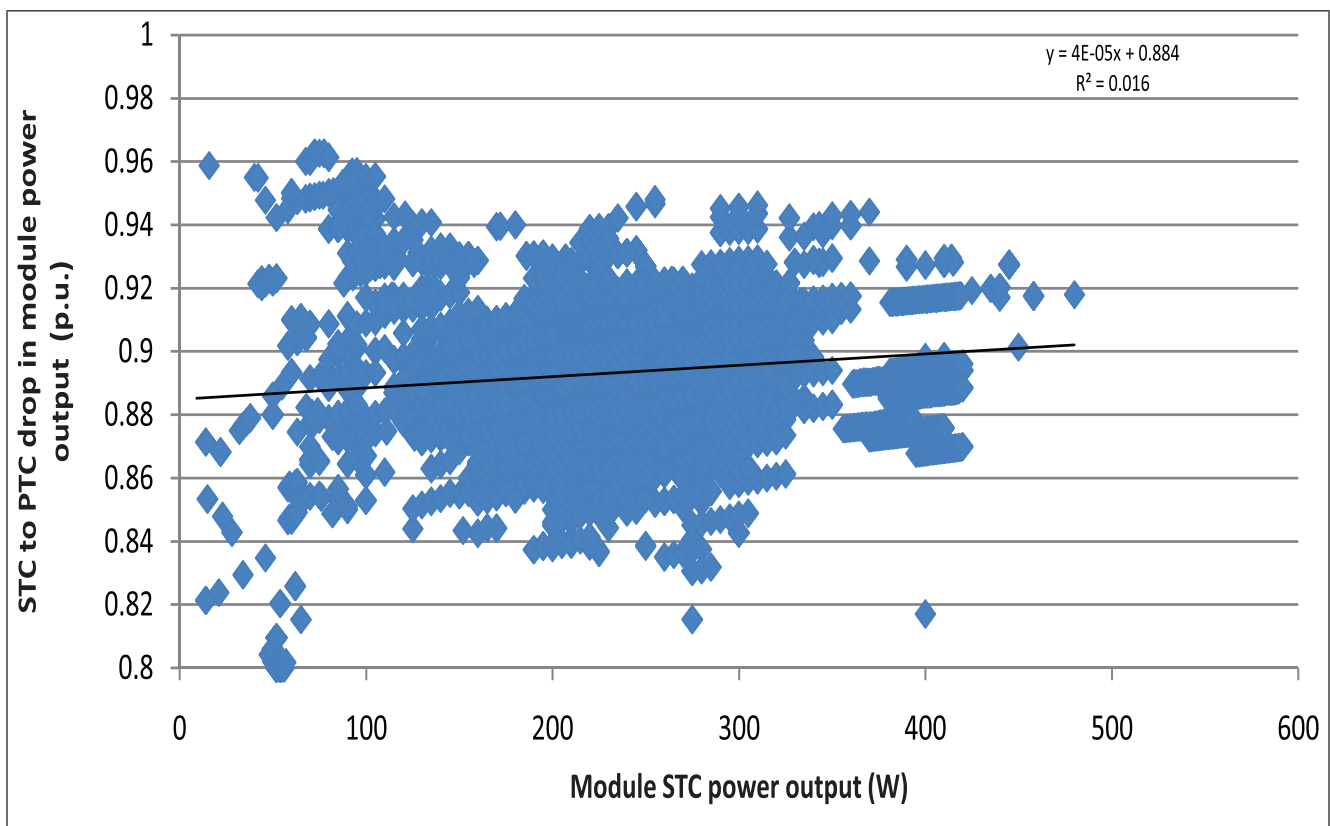
FIG. 4   DROP IN MODULE POWER OUTPUT FROM STC TO PTC FOR OVER 16,000 DATA POINTS

3.3   Effect of temperature, temperature coefficients and temperature induced efficiency drop.

In real life operation, cell temperature is one of the main parameters in which the cell deviates from the STC operating condition and the effect of temperature is quantified by the temperature coefficients (%/°C)   for various cell and module operational and performance parameters.

Fanney *et al.* [20] have compared the performance of module and cell temperature coefficients (%/°C)   for C-Si, M-Si and A-Si modules   in respect of VOC, ISC and Pmax. They have also considered the effects of air mass and incident angle. Temperature coefficients (%/°C)   in respect of VOC, ISC and Pmax , FF have been established for A-Si and other thin film modules [21].   For outdoor performance monitoring the role of performance coefficients has been highlighted as a mode of ensuring that the annual data is within predefined accuracy limits [22].

The influence of temperature coefficients and solar sky spectrum on the performance of C-Si and A-Si cells have been analyzed by Karki and   Faiman [23]. Spectral sensitivity affects the temperature coefficients. A detailed review of the temperature dependence on the efficiency and power of SPV cells has been conducted by Skoplaki and Palyvos [24].

Losses due to accumulation of dust have been studied considering both masking as well as incident angle change in areas with rain and without rain [25]. The quantification of irradiance loss has been modeled for the whole day and shown to be as high as 14.8 % [25].

3.4   Maximum power point tracking (Fill factor)

The maximum power tracking can be represented through the fill factor. The influence of no of junctions on the fill factor are given   in Figure 5 below.
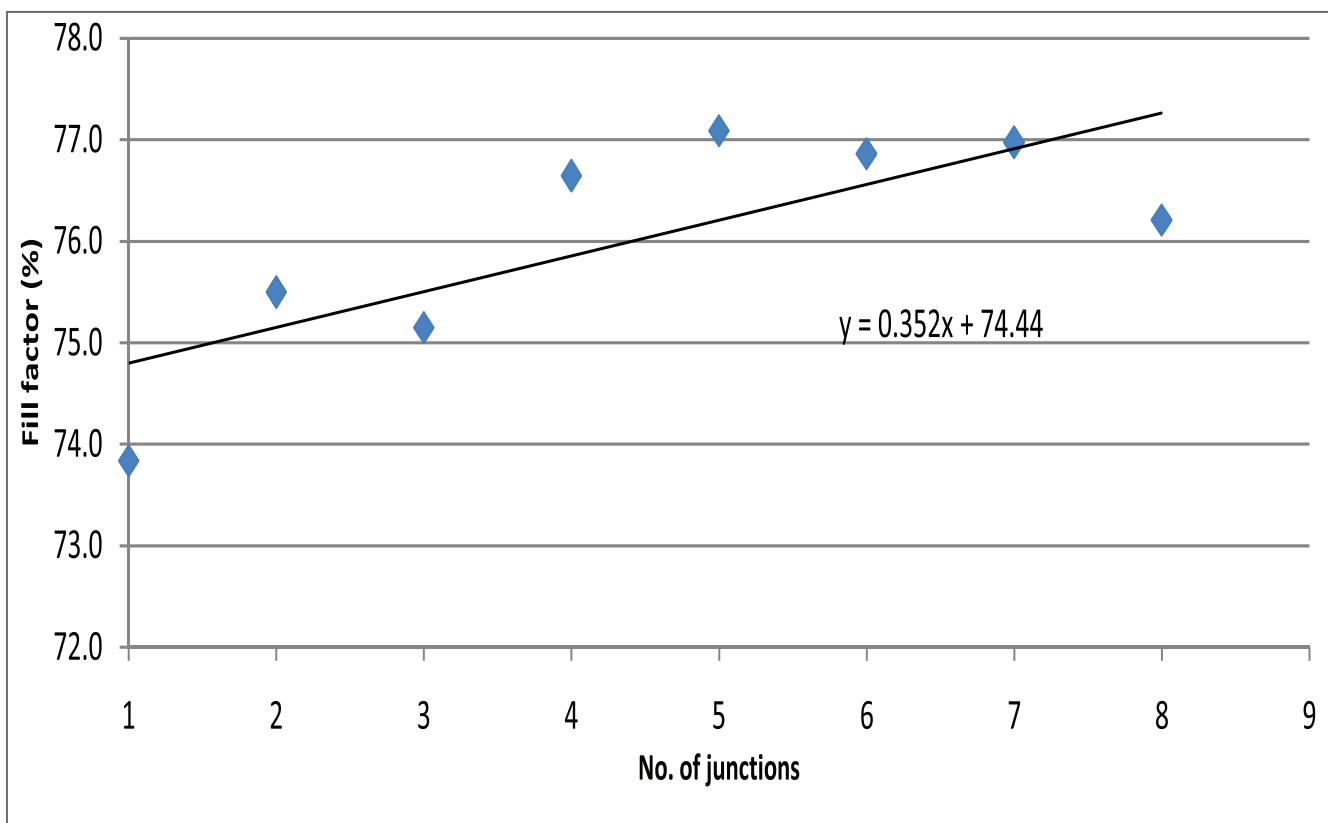

FIG. 5   INFLUENCE OF NUMBER OF JUNCTIONS ON THE FILL FACTOR

3.5 Effect of solar energy intensity -Module part load efficiency

The part load characteristics of C-Si, M-Si and A-Si modules are given in the Figure 6 below.

The efficiencies are lower in the weak light region (below 200-400 W/m^2) due to high level of spectral mismatch. There is a misconception that A-Si performs better in the weak light region as compared to C-Si and M-Si. This is not true in view that the efficiency of A-Si does not come anywhere near the efficiency of C-Si or M-Si even though its weak light performance is better.
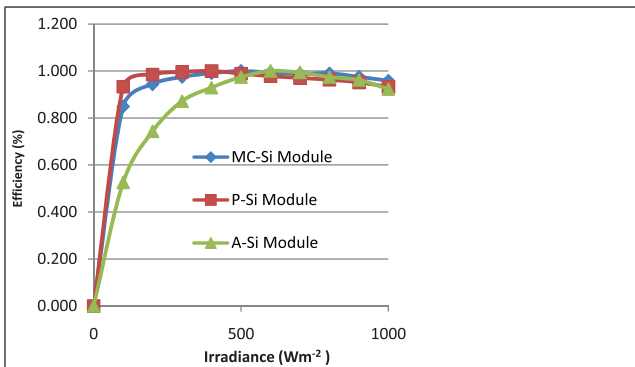

FIG. 6   PART LOAD EFFICIENCY CHARACTERISTICS OF C-Si, M-Si AND A-Si MODULES

3.6 Effect of environmental parameters-RH, wind speed and air mass

A decrease in performance is noted with increase in air mass, turbidity and water vapour in the air [26].

Sarver *et al.* [27] have comprehensively review the effect of dust and soiling on the performance of SPV modules. The dust material, particle size and deposited layer density has an effect on the efficiency of the modules. Restorative, preventive and mitigation approaches have been adopted for restoring the performance. The impact of natural soiling on transmission efficiency of the SPV cover plate has been quantified [28]. Transmission efficiency has been reduced to 89 to 96 % as compared to a clean condition. The effect of air mass function has been quantified in terms of the temperature coefficients [20]. Even though temperature coefficients by air mass function varied by as much as 17 % the impact on efficiency was only 2 % [20]. King [22] has developed correlations between STC performance to outdoor array performance. The array performance model considers the environmental parameters such as incident angle, solar spectrum, absolute air mass and wind speed [22]. The correlation between the module temperature rise and the wind speed (m/s) below 18 m/s, is as follows [22]:

$$\frac{T_{mod} - T_0}{P_I} = 0.0712v^2 - 2.411v + 32.96 \qquad ....(5)$$

The quantification of the effects of dust thickness, turbidity, water vapour and air mass are given in the Figures 7-10 below [26].
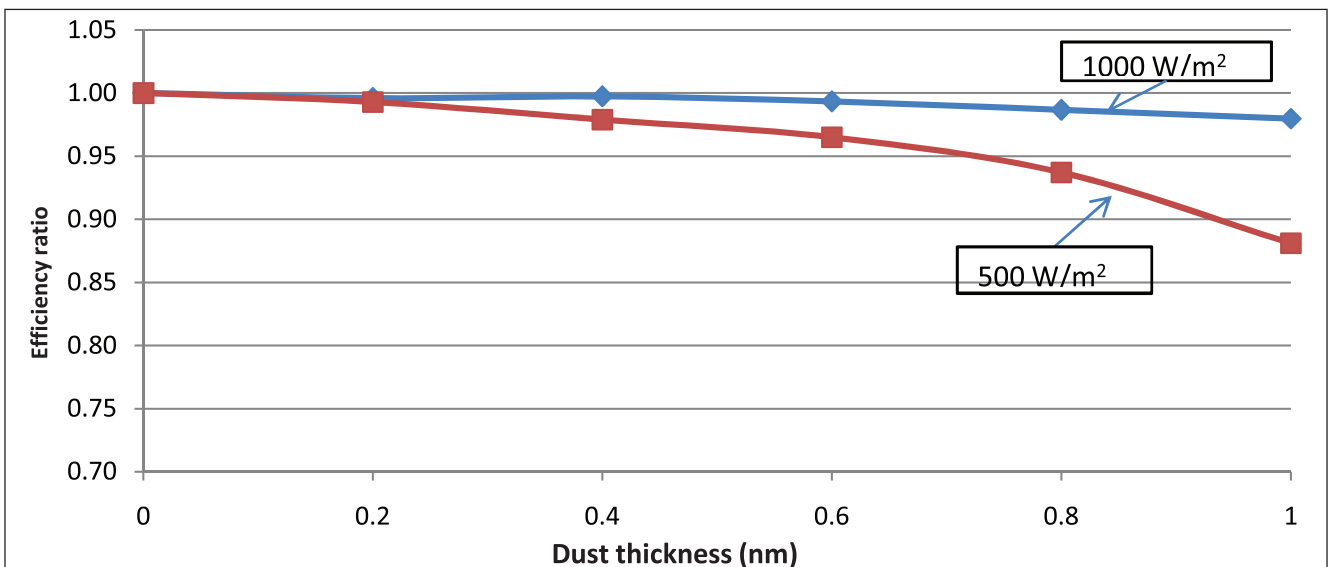

FIG. 7   EFFECTS OF DUST THICKNESS ON RELATIVE EFFICIENCY [26]
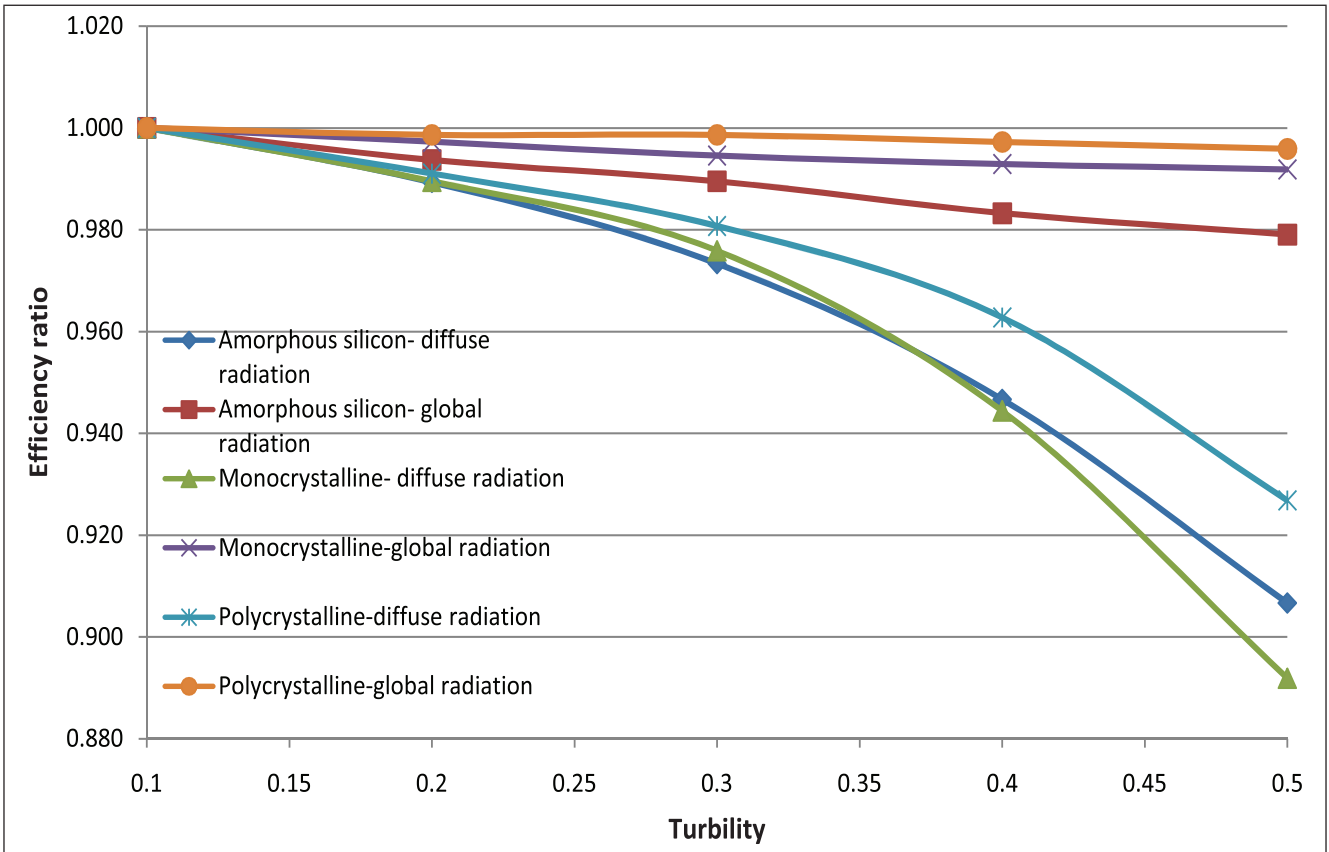
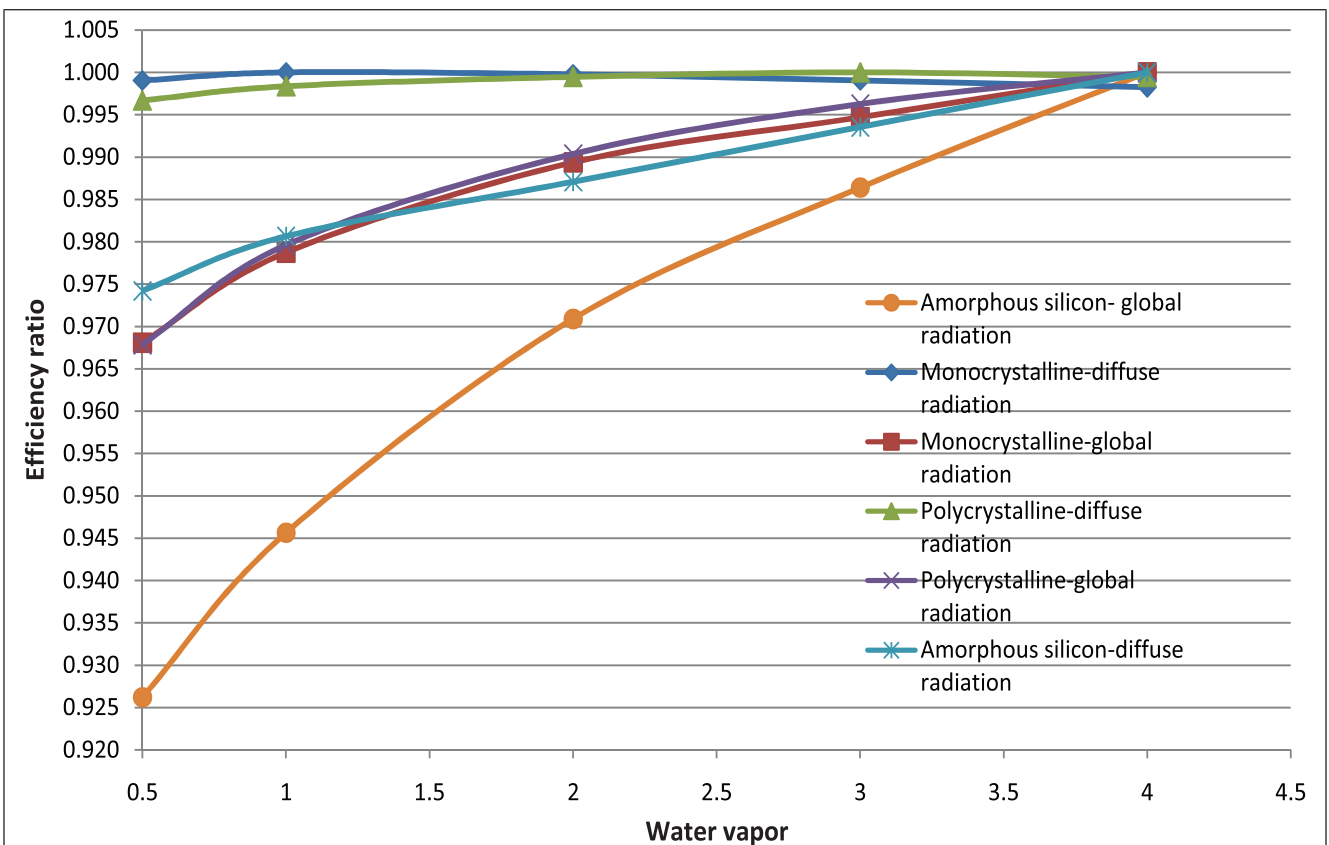FIG. 8   EFFECTS OF TURBIDITY ON RELATIVE EFFICIENCY [26]

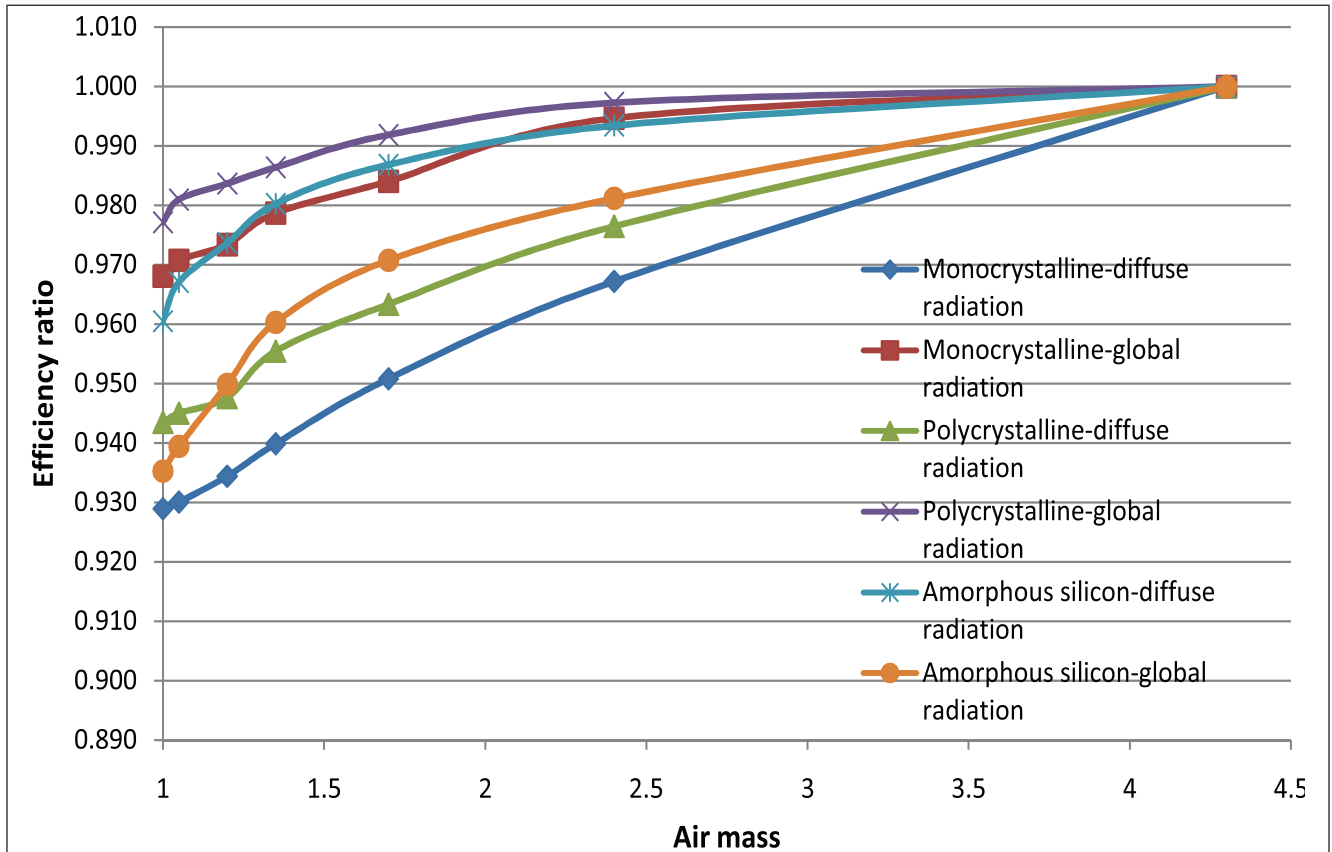FIG. 9   EFFECTS OF WATER VAPOUR ON RELATIVE EFFICIENCY [26]

FIG. 10 EFFECTS OF AIR MASS ON RELATIVE EFFICIENCY [26]

One of the   prominent indicators of the environmental effects such as cloud cover, turbidity, fog, water vapour, etc., is the stochastic efficiency.

TABLE 2				
STOCHASTIC EFFICIENCY OF SOLAR IRRADIANCE AT FIVE LOCATIONS IN INDIA				
Sl. No.	Location	Annual Radiation (kWh/ m²year)	Max Radiation per day (kWh/ m²day)	Stochastic efficiency (%)
1	Bangalore	1744.6	7.3	65.6
2	New Delhi	1781.3	7.7	63.0
3	Kolkata	1748.8	6.6	72.3
4	Mumbai	1892.8	7.2	72.0
5	Chennai	1789.4	7.1	69.5

This is the ratio of the annual irradiance in an year to the maximum irradiance in an year (i.e., maximum energy generation in a day in a given year x 365). The solar irradiance is continuously fluctuating with duration of 10 s to few minutes due to cloud movement, appearance

of cloud cover, cloud reflection, etc. The small time fluctuation of below 10 s dues not affect the efficiency seriously.

It can be seen that the stochastic efficiency is around 63 % to 73 % in the four metros and Bengaluru (Table 2). It is of the order of 85 % in the scanty rainy regions like Rajasthan.

3.7   Effect of module tracking and incident angle of irradiation

The incident angle function does not show significant effect on the performance up to 50° [20]. Beyond this level of mismatch there is a serious drop in the short circuit current [20, 22].

The solar angle of incidence is given by,

$$\theta_{incidence} = \cos^{-1}[\{\cos(\theta_{tilt})\cos(\theta_{zenith})\} + \{\sin(\theta_{tilt})\sin(\theta_{zenith})\cos(\theta_{azimuth\ sum} - \theta_{azimuth\ module})\}]$$

....(6)

$\theta_{incidence}$ = Solar angle of incidence (deg)

θ_{tilt} = Tilt angle of module (deg) (0^0 is horizontal)

θ_{zenith} = Zenith angle of sun (deg)

$\theta_{azimuth\ sum}$ = Azimuth angle of sun (0^0 = North, 90^0 = East)

$\theta_{azimuth\ module}$ = Azimuth angle of module (0^0 = North, 90^0 = East)

Physical sun tracking of SPV modules has shown improvement of 15-36 % in the total energy yield on an annual basis [29].

3.8   Effect of cell resistance- series and shunt

For 150 mm cells, the lowest shunt resistance (R_{SH}) is 4.5 Ω [30]. As the shunt resistance increases the performance improves. The cell performance is mainly affected in the weak light of below 400 W/m² [30]. Above 400 W/m² the effect is very little. The saturation values for R_{SH} are 20-30 Ω for 150 mm cells. In practice R_{SH} can range between 2-200 Ω for 150 mm cells [30]. Shunt resistance can affect the annual energy yield by as much as 5-30 % [30].

3.9   Degradation characteristics

Degradation can be classified as:

- Light induced degradation (initial degradation)
- Potential induced degradation
- Ageing degradation

A detailed study on power loss on initial degradation of C-Si modules indicated a drop of 1.7 to 3.4 % with an average loss of 2.4 % during the first season of exposure [31]. In C-Si the initial power loss for the first 60-100 h is around 1-4 % while in M-Si cells it is around 1 % [32].

A-Si modules demonstrate degradation in three distinct phases- an initial phase of 10-20 hours show around 12-13 %, a middle phase of 60-100 h showing a further drop of 10-12 % and a slower phase of long term degradation of 10-12 % over a period of 20-30 days [33]. Prolonged soaking in light resulting in decrease of conductivity of amorphous silicon cells is termed as the Staebler-Wronski effect. This is caused by thermal annealing of the cells after around 1 khours of soaking in light leading to an efficiency drop of 10-30 %. The annual long term degradation rate of A-Si is 0.79 % [19].

Ageing degradation of efficiency (~ -1 %/year) with time is a factor which needs to be kept in check [34-35]. Degradation is linked to operation and maintenance practices and superiority in these areas can contain degradation to -0.25 %/year [35].

3.10 Effect of no of junction

Multi junction cells have long been considered as avenues for efficiency enhancement. Doeleman [36] has worked out the efficiencies of multi junction cells using the detailed balance model. He has concluded that above 5 cell junctions the efficiency increase per junction less around 2 % and hence it is unfeasible to go beyond 5 junction cells. The study [36] provides details of the losses in cells.

Multi-junction cells develop 1.2 % power gain in tropical zone and 3.4 % in arctic zone [37].

Under non concentration conditions cell efficiency is increased by 40 % through multi-junctions. The overall module efficiency increased from 10.81 % to 12.63 % [38]. Multi-junction solar cells with II-IV, III-IV material designs recorded higher efficiencies.

The variation in ultimate efficiency, detailed balance efficiency, maximum conversion efficiency and SQ efficiency of cells for multi junction cells given by Doeleman [36] are shown in Figure 11.
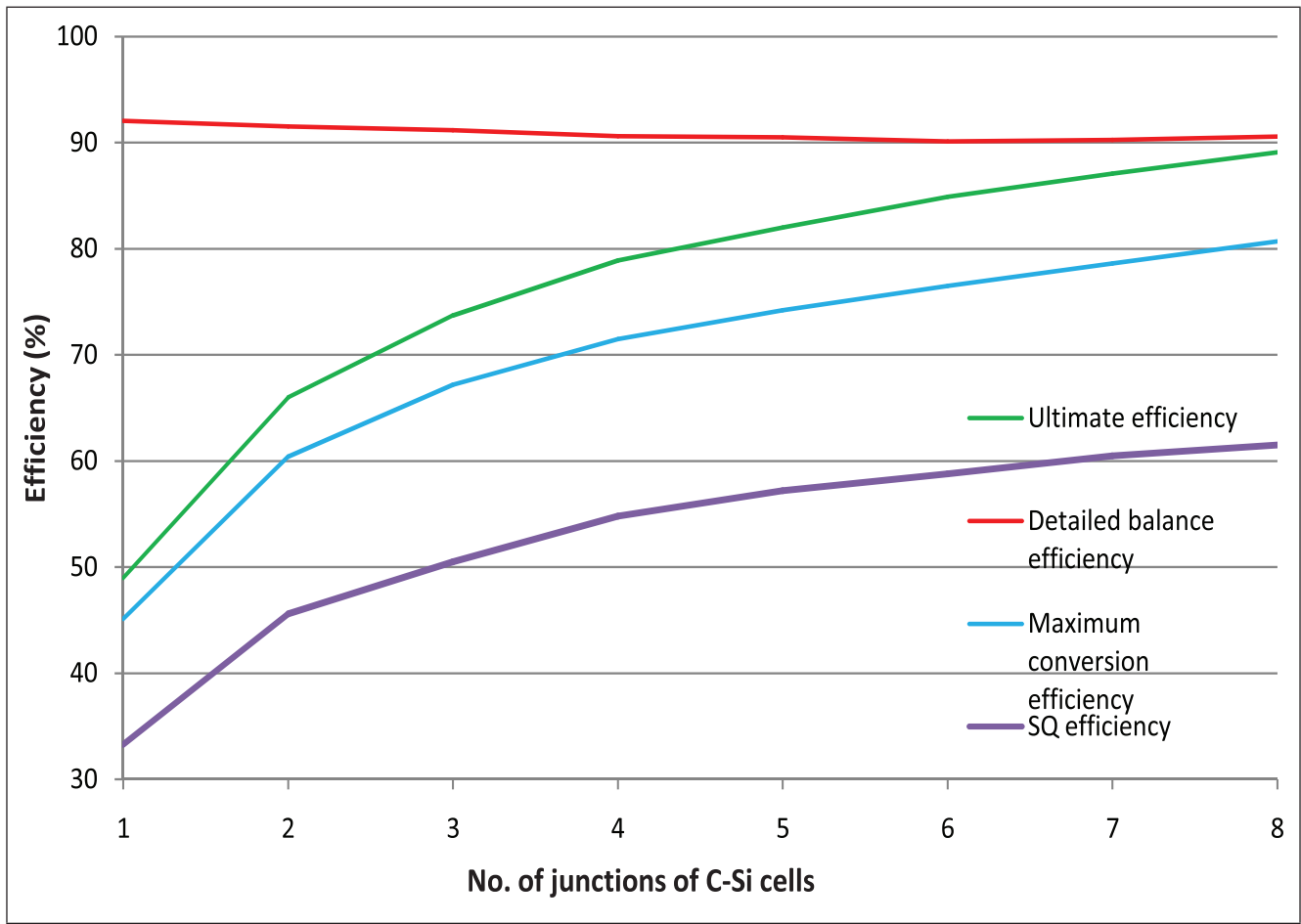
FIG. 11   EFFECTS OF TURBIDITY ON RELATIVE EFFICIENCY [26]

3.11 Effect of architecture organization into module, panel, array and system

Based on the modular architecture of SPV systems, from the cell to the module, from module to array and array to a plant, there is drop in conversion efficiency due to losses in each system. Normally for practical purposes cell efficiencies cannot be considered in isolation because the cell has to packaged into the module. Generally, energy efficiency is represented and compared for the module. For the array or the plant, a term called Performance Ratio (PR) is used. Baltus *et al.* (1997) [37] have measured SPV system losses, represented them through a Sankey's diagram and used Performance Ratio (PR) to relate the measured overall system efficiency to the module efficiency [37]. The PR is measured to be in the range of 0.612 to 0.737. The PR [3] is defined as:

$$PR = \left[\left(\frac{E_{actual,\ output}}{E_{actual,\ irradiance}} \right) \Big/ \left(\frac{\Sigma\Sigma\ E_{STC,\ output}}{\Sigma\Sigma\ E_{STC,\ irradiance}} \right) \right]_{year}$$

$$= \left[\left(\frac{E_{actual,\ output}}{\Sigma\Sigma\ E_{STC,\ output}} \right) X \left(\frac{\Sigma\Sigma\ E_{STC,\ irradiance}}{E_{actual,\ irradiance}} \right) \right]_{year}$$

$$= \left[\left(\frac{E_{actual,\ output}}{\Sigma\Sigma\ E_{STC,\ output}} \right) \Big/ \left(\frac{E_{actual,\ irradiance}}{\Sigma\Sigma\ E_{STC,\ irradiance}} \right) \right]_{year}$$

$$= \frac{Specific\ energy\ yield}{Stochastic\ efficiency} \qquad ....(7)$$

PR compares the performance of the system under actual operating conditions with that under STC conditions.   It considers the stochastic efficiency (actual irradiance/ maximum possible irradiance in the given location).

Modeling system losses in SPV systems, [39] has classified system losses into optical, array and electrical losses and quantified these. The system

losses consisting of optical losses, electrical losses as well as due to MPPT tracking have been computed at 72 %. Electrical yield improvement in SPV modules is through computation and minimization of the optical losses [40]. The concept of avoidable losses due to faults has been proposed and measured to be in the range of 3.6 % to 58 %. Avoidable losses have been identified in the optical system (shading) and electrical circuit (inverter shut down, system isolation, etc.) [41] and represent the percentage of the system losses which could be easily avoided during system operation.

System efficiency has been used as a basis for sizing of SPV system [42-43] have modeled the system losses   like shading, incident angle dependence, load mismatch, temperature effect on cells, array electrical limit losses [43]. They have quantified the PR at 67 % for 421 sites over a period of 1995 to 1999 [43].

MPPT mismatch losses have been quantified in arrays. The effects of shading and string configuration have also been considered in the mismatch [44].

Optimization of balance of system as a route for improving the overall efficiency has been advocated [45]. Alternative approach to evaluation of PR is through non-module system efficiency [46].

Table 3 gives the drop in module efficiency as compared to the cell efficiency for C-Si and M-Si. Figure 12 gives the drop between the module and cell efficiency for C-Si and M-Si. It can be seen that the drop is between 2 to 3 % point.
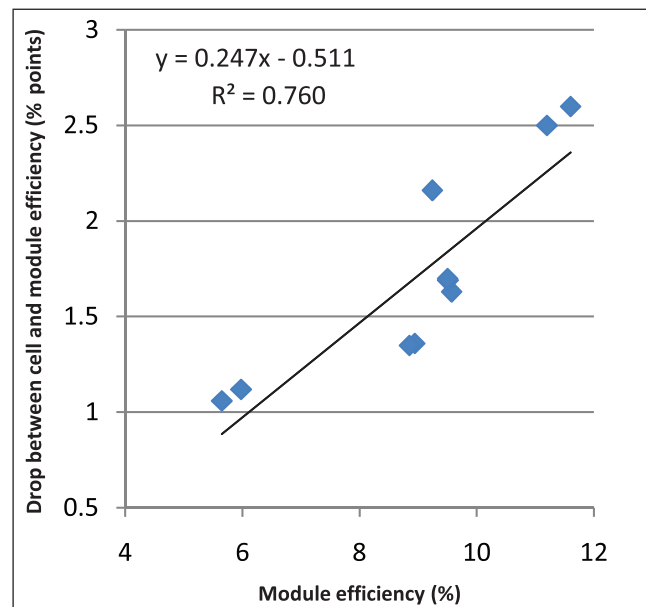

FIG. 12   DROP BETWEEN THE MODULE AND CELL
EFFICIENCY FOR C-Si AND M-Si.

Table 4 gives the drop in efficiency between module to array. It can be seen that the drop between the modules to array is around 3.83 % points.

TABLE 3
MODULE EFFICIENCY COMPARISION FOR C-SI AND M-SI

Sl. No.	Particulars	Min	Max
1	Cell efficiency	18.6	18.6
2	Module loss	0.84	0.89
3	Module efficiency	15.62	16.55
4	Module efficiency drop (% points)	3.0	2.0

TABLE 4
DROP IN EFFICIENCY BETWEEN MODULE TO ARRAY

Sl. No.	Particulars	Value
1	Module efficiency (PTC)	15.6
2	SPV module name plate de-rating	0.95
3	Inverter and transformer losses	0.92
4	Module mismatch	0.98
5	Diodes and connections	0.995
6	DC wiring	0.98
7	AC wiring	0.99
8	Dust and radiation transmission losses	0.95
9	System availability	0.98
10	Shading in the site	0.98
11	Sun-tracking	1
12	Module to array de-rating	0.75
13	Array efficiency	11.77
14	Module to array drop	3.83

4.0 EFFECT OF CONCENTRATION RATIO OF SOLAR IRRADIATION

Besides multi junction cells, concentration is another important area of SPV performance boosting. Messmer [47] has shown that concentrated SPV modules with two axis tracking can give efficiencies of around 30 %. The role of anti reflective coatings in enhancing efficiency of concentrated SPV modules and its impact on capital cost has also been highlighted. In concentrating SPV cells, as the concentrating ratio (CR) increases from 1 to 200 cell efficiency increases from 29.5 % to 37.0 % [47]. But concentration results in temperature rise (25 to 140 °C) which leads to drop in cell efficiency by 2.5 % points for CRs of 200 to 10 % points for CR of 1 [47]. Systems for heat dissipation or withdrawal are required to keep the cell temperatures within 10 °C of the ambient temperature. The effect on concentration in multi junction cells have been studied by Doeleman [36] and shown that the efficiency increases from 30.7 % for unconcentrated cells to 38.3 % for concentration of 10^3 suns. A disadvantage of concentration besides temperature coefficient is the deterioration of the cell structure due to thermal stress and fatigue.

The variation of SQ efficiency for single junction cells with concentration is given in the following Figure 13.

5.0 DISCUSSION

While specification of the power output of a photovoltaic plant for evaluation during acceptance testing, care must be taken to indicate the point at which the measurement is taken (sum total of module outputs, sum total of string outputs, array output DC or AC) and the time period for the same. The measurement of module outputs do not provide the array output. Further the array output on the load side (AC) must be considered.
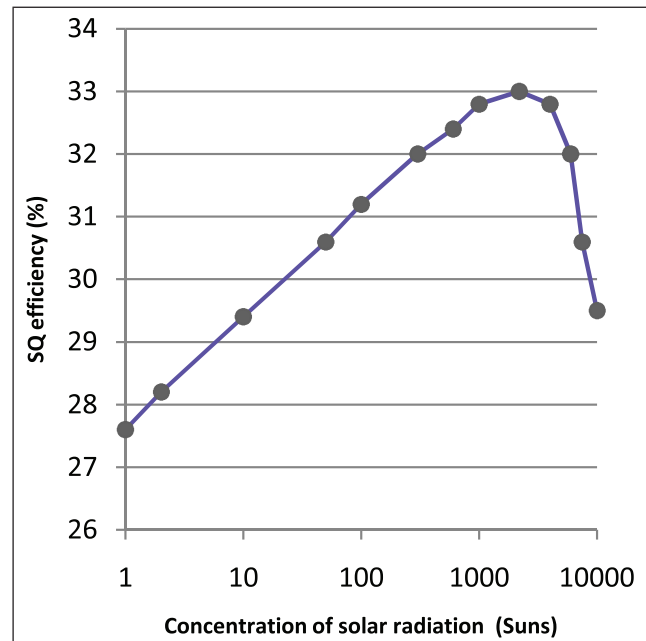

FIG. 13 VARIATION OF SQ EFFICIENCY FOR SINGLE JUNCTION CELLS

6.0 CONCLUSIONS

1. The main conclusions of this study are as follows:

   i.   A rational classification of the losses in SPV systems is required for understanding the various components which lead to the losses. The losses in the SPV system can be classified as:

   ii. Losses in the cell which lowers the ultimate SQ efficiency to the nominal SQ efficiency. Many of these losses can be overcome only in the design and manufacturing stage.

   iii. Drop in efficiency from the cell SQ efficiency to the module efficiency under STC conditions. These losses depend on the efficacy of module manufacture from the cells.

   iv. Drop in efficiency of modules due to deviation from STC conditions to actual operating conditions. These losses are operation and maintenance dependent.

   v.   Performance ratio which includes drop in efficiency from module to array and which includes stochastic efficiency of the site under consideration. These losses include partially the non module

system efficiency and partially losses due connection to the load or the grid.

2. The effect of environmental parameters, no of junctions, solar concentration (no of suns), etc., on the performance of systems has been quantified.

REFERENCES

[1]   E Rephaeli and S Fan, Absorber and emitter for solar thermo-photovoltaic systems to achieve efficiency exceeding the Shockley-Queisser limit, Optics Express, Vol. 17, pp. 15145-15159, 2009.

[2]   M A Green, K Emery, Y Hishikawa and W Warta, Solar cell efficiency tables, progress in photovoltaics: research and applications, Vol. 37, pp. 84-92, 2010.

[3]   N Aste, C D Pero, F Leonforte, PV technologies performance comparison in temperate climates, Solar Energy, Vol. 109, pp. 1–10, 2014.

[4]   J Nelson and J Kirkpatrick, Analysis of the photovoltaic efficiency of a molecular solar cell based on a two-level system. Applied Physics A: Materials Science and Processing, Vol. 79, No. 1, pp. 15-20, 2004.

[5]   D P Soldan, A Lee, S M Thon, M M Adachi, H Dong, P Maraghechi, M Yuan, A J Labelle, S Hoogland, K Liu, E Kumacheva and E H Sargent, Jointly tuned plasmonic–excitonic photovoltaics using nanoshells, Vol. 13, No. 4, pp. 1502-1508, 2013.

[6]   K Nishioka, T Takamoto, T Agui, M Kaneiwa, Y Uraoka and T Fuyuki, Evaluation of InGaP/InGaAs/Ge triple-junction solar cell and optimization of solar cell's structure focusing on series resistance for high-efficiency concentrator photovoltaic systems, Solar Energy Materials and Solar Cells, Vol. 90, No. 9, pp. 1308-1321, 2006.

[7]   Y Zhao, M Y Sheng, W X Zhou, Y Shen, E T Hu, J B Chen, M Xu, Y X Zheng, Y P Lee, D W Lynch and L Y Chen, A solar photovoltaic system with ideal efficiency close to the theoretical limit, Optics Express, Vol. 20, No. 1, pp. 28-38, 2012.

[8]   E Rephaeli and S Fan, Absorber and emitter for solar thermo-photovoltaic systems to achieve efficiency exceeding the Shockley-Queisser limit, Optics Express, Vol. 17, pp. 15145-15159, 2009.

[9]   D Yang and H Yin, Energy conversion efficiency of a novel hybrid solar system for photovoltaic, thermoelectric, and heat utilization, Art. no. 5738324, Energy Conversion, IEEE Transactions on Vol. 26, No. 2, pp. 662-670, 2011.

[10] A H Nosrat, L G Swan and J M Pearce, Improved performance of hybrid photovoltaic-trigeneration systems over photovoltaic-cogen systems including effects of battery storage, Energy, Vol. 49, pp. 366-374, 2013.

[11] A Buonomano, F Calise, M D d'Accadia and L A Vanoli, A Novel solar trigeneration system based on concentrating photovoltaic/thermal collectors. Part 1: Design and simulation model, Energy, Vol. 61, pp. 59–71, 2013.

[12] A Joyce, L Coelho, J Martins, N Tavares, R Pereira and P Magalhaes, A PV/t and heat pump based trigeneration system model for residential applications, Kassel Conference: ISES - Solar World Congress at Kassel, 2011.

[13] J N Munday, The effect of photonic bandgap materials on the Shockley-Queisser limit, Journal of applied physics, Vol. 112, pp. 1-6, 2012.

[14] B Liao and W C Hsu, An investigation of Shockley-Queisser limit of single p-n junction solar cells, Rep 2.997, MIT, Cambridge, MA 2011, pp. 1-11.

[15] Miro Zemon, in Handbook of Solar Cells, pp. 5.11-5.12

[16] C J Chen, Physics of solar energy, Department of Applied Physics and Applied Mathematics Columbia University, John

Wiley & Sons, Inc., Hoboken, New Jersey, pp. 1-373, 2011.

[17] A R Jha, Solar cell technology and applications, CRC Press, Auerbach Publications, Taylor & Francis Group, 6000 Broken Sound Parkway NW, Suite 300 Boca Raton, pp. 1-280, 2010.

[18] ASTM standard G 197-08, Standard table for reference solar spectral distributions: direct and diffuse on 20° tilted and vertical surfaces, ASTM International, 100 Barr Harbor Drive, West Conshohocken, United States, pp. 1-21, 2008.

[19] K Agroui, A H Arab, M Pellegrino, F Giovanni and I H Mahammad, Indoor and outdoor photovoltaic modules performances based on thin films solar cells, Revue des Energies Renouvelables, Vol. 14 No. 3, pp. 469-480, 2011.

[20] A H Fanney, M W Davis, B P Dougherty, D L King, W E Boyson, J A Kratochvil, Comparison of photovoltaic module performance measurements, Journal of Solar Energy Engineering, Transactions of the ASME, Vol. 128, pp. 152-159, May 2006.

[21] A Virtuani, D Pavanello and G Friesen, Overview Of temperature coefficients of different thin film photovoltaic technologies, Scuola Universitaria Professionale della Svizzera Italiana (SUPSI) Istituto per la Sostenibilità Applicata all'Ambiente Costruito (ISAAC), Canobbio CH-6952, Switzerland, pp. 01-05.

[22] D L King, Photovoltaic module and array performance characterization methods for all system operating conditions, Proceeding of NREL/SNL Photovoltaics Program Review Meeting, New York, pp. 01-22, Nov.1996.

[23] I B Karki and D Faiman, Solar spectral influence on the performance of crystalline based photovoltaic modules under hot weather, Scientific World, Vol. 11, No. 11, pp. 48-51, July 2013.

[24] E Skoplaki and J A Palyvos, On the temperature dependence of photovoltaic module electrical performance: A review of efficiency/power correlations, Solar Energy, Vol. 83, pp. 614–624, 2009.

[25] J Z Casanova, M Piliougine, J Carretero, P Bernaola, P Carpena, L M Lopez, and M S Cardona, Analysis of dust losses in photovoltaic modules, World renewable energy congress, Sweden, pp. 2985-2992, 2011.

[26] M Chegaar, P Mialhe, Effect of atmospheric parameters on the silicon solar cells performance, Journal of Electron Devices, Vol. 6, pp. 173-176, 2008.

[27] T Sarver, A A Qaraghuli, L L Kazmerski,A comprehensive review of the impact of dust on the use of solar energy: History, investigations, results, literature, and mitigation approaches, Renewable and Sustainable Energy Reviews, Vol. 22, pp. 698–33, 2013.

[28] L Boyle, H Flinchpaugh, M P Hannigan, Natural soiling of photo voltaic cover plates and the impact on transmission,Renewable Energy, Vol. 77, pp. 166–173, 2015.

[29] W Durisch, B Bitnar, J C Mayor, H Kiess, K H Lam and J Close, Efficiency model for photovoltaic modules and demonstration of its application to energy yield estimation, Solar Energy Materials & Solar Cells, Vol. 91, pp. 79–84, 2007.

[30] P Grunow, S Lust, D Sauter, V Hoffmann, C Beneking, B Litzenburger and L Podlowski, Weak light performance and annual yields of PV modules and systems as a result of the basic parameter set of industrial solar cells, 19th European Photovoltaic Solar Energy Conference, pp. 2190-2193, 7-11 June 2004.

[31] A Colli, J Vasquez, W J Zaaiman, Initial stabilization of a statistical sample of forty-four mono crystalline photo voltaic modules, Renewable Energy, Vol. 75, pp. 326 – 334, 2015.

[32] M A Munoz, F Chenlo and M C Alonso-García, Influence of initial power stabilization over crystalline-Si photovoltaic modules maximum power, Progress in

photovoltaics: Research and Applications, Vol. 19, pp. 417-422, 2011.

[33] C P Lund, K Luczak, T Pryor, J C L Cornish, P J Jennings, P Knipe and F Ahjum, Field and laboratory studies of the stability of amorphous silicon solar cells and modules, Renewable Energy , Vol. 22, pp. 287 – 294, 2001.

[34] M S Bhatt, and R Sudhir Kumar, Performance analysis of solar photovoltaic plants-experimental results, International Journal of Renewable Energy Engineering, Vol. 2, No. 2, pp. 184-192, 2000.

[35] M S Bhatt, Performance evaluation of solar photovoltaic arrays after 18 years of field operation, international journal of Green Energy, Taylor & Francis, DOI: 10.1080/15435075. 2011.647169 Online: 30 Apr 2012.

[36] H Doeleman, Limiting and realistic efficiencies of multi-junction solar cells, Photonic Materials Group, FOM institute AMOLF, Amsterdam, pp. 1-33, 2012.

[37] C W A Baltus, J A Eikelboom, and R J C Zolingen, Analytical monitoring of losses in pv systems, Paper presented at the 14th European Photovoltaic Solar Energy Conference Barcelona [ftp://ftp.ecn.nl/pub/www/library/report/1997/rx97043.pdf], pp. 1-5, June 1997.

[38] Y Su, L C Chan, L Shu and K Tsui, Real-time prediction models for output power and efficiency of grid-connected solar photovoltaic systems. Applied Energy, Vol. 93, pp. 319-326, 2012.

[39] A Mermoud, Modeling systems losses in PV syst, Institute of the Environmental Sciences/Group of Energy/PV syst. University of Geneva [http://www.docseek.net/mmrtyv/mermoud-pvsyst-thu-840-am.html], pp. 1-15, 2012.

[40] D Doble, Approaches to energy yield improvement in PV Modules, Fraunhofer Center for Sustainable Energy Systems, Presented at   Intersolar North America [http://cse.fraunhofer.org/Portals/55819/docs/energy-yield-improvement-intersolar-2010.pdf], pp. 1-19, July 2010.

[41] S K Firth, K J Lomas and S J Rees, A simple model of PV system performance and its use in fault detection, Solar Energy, Vol.84, pp. 624–635, 2010.

[42] Anon, Grid-tied photovoltaic system sizing, harmony farm solar [http://www.harmony   farmsupply.com/wp-content/uploads/2010/12/Photovoltaic-Solar-System-Sizing.pdf], pp. 1-2, 2012.

[43] T Oozeki, T Izawa, K Otani, and K Kurokawa, An evaluation method of PV systems, Solar Energy Materials & Solar Cells, Vol.75, pp. 687–695, 2003.

[44] B P Koirala, B Sahan, and N Henze, Study on MPP mismatch losses in photovoltaic applications, Department of Electrical Engineering, Malaviya National Institute of Technology Jaipur [http://www.docstoc.com/docs/135619823/study-on-mpp-mismatch-losses-in-photovoltaic], pp. 1-7, 2012.

[45] H Robertson, Optimizing photovoltaic systems: recent developments in system components make a significant impact on solar efficiency, Electronic Products (Garden City, New York), Vol. 52, No. 4, 2010.

[46] M S Bhatt, System Efficiency (non-module) considerations in the sizing solar photovoltaic plants" Journal of CPRI, Vol. 10, No. 02, pp. 345-354, June 2014.

[47] E R Messmer, Solar cell efficiency vs module, power output: simulation of a solar cell in a CPV module, solar cells - research and application perspectives, pp. 307-326, March 2013.